Supporting information: Effect of stoichiometry on crosslinked epoxy resin characteristics: Structural heterogeneities, topological defects, properties, free volume and segmental mobilities

Arun Srikanth Sridhar[a]

[a]Department of fiber and polymer technology, The Royal Institute of Technology (KTH), 10044 Stockholm, Sweden

Contents

S1 Estimation of T_g **6**

S2 Regression models used for estimating missing properties from experimental data **19**

S3 Data availability **22**

List of Figures

S1 Chemical reaction between epoxy and amine precursors (a) primary amine reaction (b) secondary amine reaction. (c) etherification 3

S2 Partial atomic charges that were reassigned when a secondary amine was formed. 4

S3 Partial atomic charges that were reassigned when a tertiary amine was formed. 4

S4 Average density as a function of temperature. Uncertainties are smaller than the symbols . . 5

S5 Volume as a function temperature for the systems studied. The black lines represent the linear fit to the rubbery and glassy regime. 5

S6 Illustration of T_g estimation procedure. $(\bar{T_{gl}}, \bar{\rho_{gl}})$ and $(\bar{T_r}, \bar{\rho_r})$ are the centroids of the glassy line segment (red) and the rubbery line segment (blue) respectively. T is the temperature, ρ is the density and T_g is the glass transition temperature. 7

S7 C-N bonds created at each cure iteration in R=0.4 samples 8

S8 C-N bonds created at each cure iteration in R=0.67 samples 9

S9 C-N bonds created at each cure iteration in R=1 samples 10

S10 C-N bonds created at each cure iteration in R=2 samples 11

S11 C-N bonds created at each cure iteration in R=3 samples 12

S12 Concentration profiles of functional groups during cure in R=0.4 samples. The green line represents the first order kinetic fit to secondary amine evolution. 13

S13 Concentration profiles of functional groups during cure in R=0.67 samples. The green line represents the first order kinetic fit to secondary amine evolution. 13

S14 Concentration profiles of functional groups during cure in R=1 samples. The green line represents the first order kinetic fit to secondary amine evolution. 14

S15 Concentration profiles of functional groups during cure in R=2 samples. The green line represents the first order kinetic fit to secondary amine evolution. 15

S16 Concentration profiles of functional groups during cure in R=3 samples. The green line represents the first order kinetic fit to secondary amine evolution. 15

S17 Sum of the squared errors as a function of $\overline{k_2/k_1}$ for the systems studied 16

S18 Experimental data on ρ_{300} (room temperature density) as a function of amine composition (reprinted here with permission from reference [1], copyright 1999 John Wiley & Sons.). . . . 18

S19 Experimental data on linear thermal expansion coefficient in the rubbery state α_{rl} as a function of amine composition (reprinted here with permission from reference [2], copyright 1992 John Wiley & Sons). 19

S20 Fractional free volume as a function of temperature for the systems studied. 21

S21 Average fractional free volume as a function of temperature for the systems studied. The temperature range over which crossover in the trend i.e., increase in fractional volume to decrease in fractional volume, for deviations from R=1, occurs is shown. 22

S22 Experimental data on linear thermal expansion coefficient in the rubbery state α_{rl} as a function of amine composition (reprinted here with permission from reference [2], copyright 1992 John Wiley & Sons). 22

List of Tables

S1 Formulations studied in this work 3

S2 Temperature ranges used for the estimation of T_g and CVTEs 17

S3 Simulation box specifications: × stands for crosslinking. The simulation box is cubic. Uncertainties in box lengths are negligible. 17

S4 Monomer types in R=0.4 system. 17

S5 Monomer types in R=0.67 system. 17

S6 Monomer types in R=2 system. 17

S7 Monomer types in R=3 system. 18

S8 Experimental data on room temperature density ρ_{300} and glass transition temperature T_g. The values of T_g were taken from reference [1]. The density data were extracted from Fig. S18 using a graphical extraction tool [3]. The amine composition in pph was converted to an equivalent amine-to-epoxy ratio R using the relation, $r = \frac{2M_E}{M_A}\frac{w_a}{w_e}$, where M_E and M_A are the molecular weight of epoxy (375 g/mol) and amine respectively and $\frac{w_a}{w_e}$ is the amine-to-epoxy weight ratio (pph amine) 18

S9 Experimental values of α_{rl}. The data were extracted from Fig. S22 using a graphical extraction tool [3]. 19

S10 Comparison of material properties determined from MD simulations (Sim.) and experimental data (Exp.) from literature. The experimental values of material properties of off-stoichiometric systems ($R \neq 1$) were obtained (estimated) using regression models. 20

S11 The adjusted values of T_g based on shift estimated using WLF equation, T_g^{WLF} and heuristic approach, $T_g^{heuristic}$ and the estimated experimental values of T_g calculated from regression model, T_g^{exp*} (same as in Table. S10, listed here for ease of comparison) 20

S12 Volume fraction of defects, ϕ_{Def} at 300 K, weight fraction of defects, w_{Def} and weight fraction of sols, w_{sol}. 20

Amine composition (wt%)	R amine:epoxy	Molecules DGEBA:PACM
10.88	0.4	540:108
16.91	0.67	480:160
23.39	1	432:216
37.91	2	343:343
47.81	3	280:420

Table S1: Formulations studied in this work

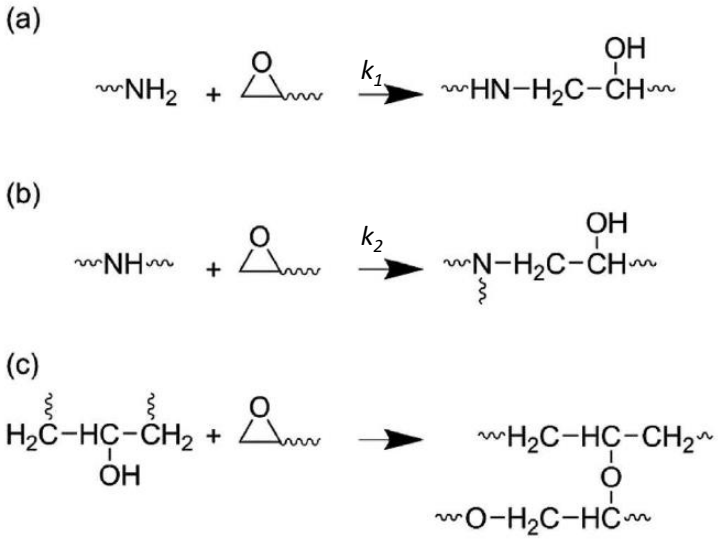

Figure S1: Chemical reaction between epoxy and amine precursors (a) primary amine reaction (b) secondary amine reaction. (c) etherification

.

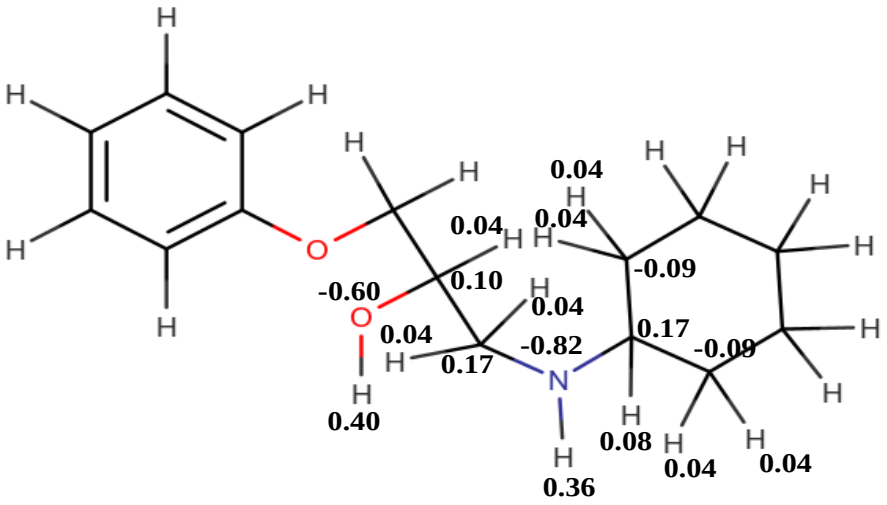

Figure S2: Partial atomic charges that were reassigned when a secondary amine was formed.

.

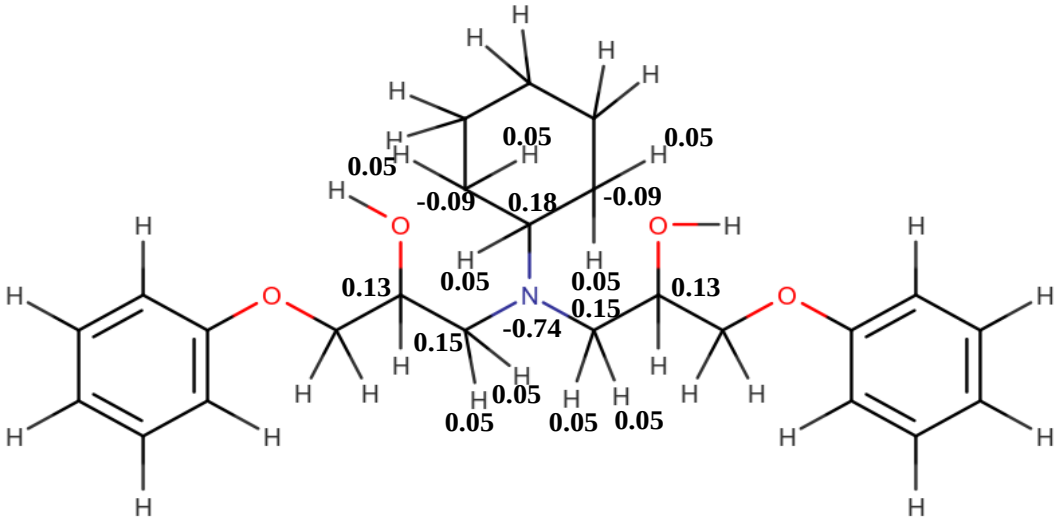

Figure S3: Partial atomic charges that were reassigned when a tertiary amine was formed.

.

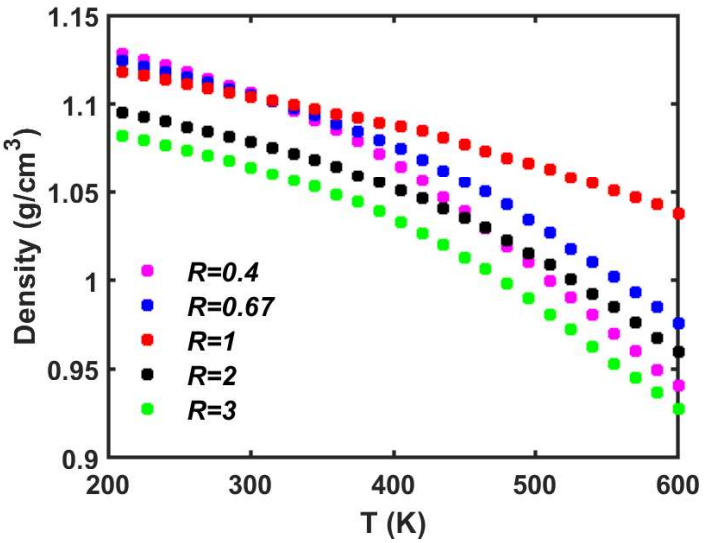

Figure S4: Average density as a function of temperature. Uncertainties are smaller than the symbols

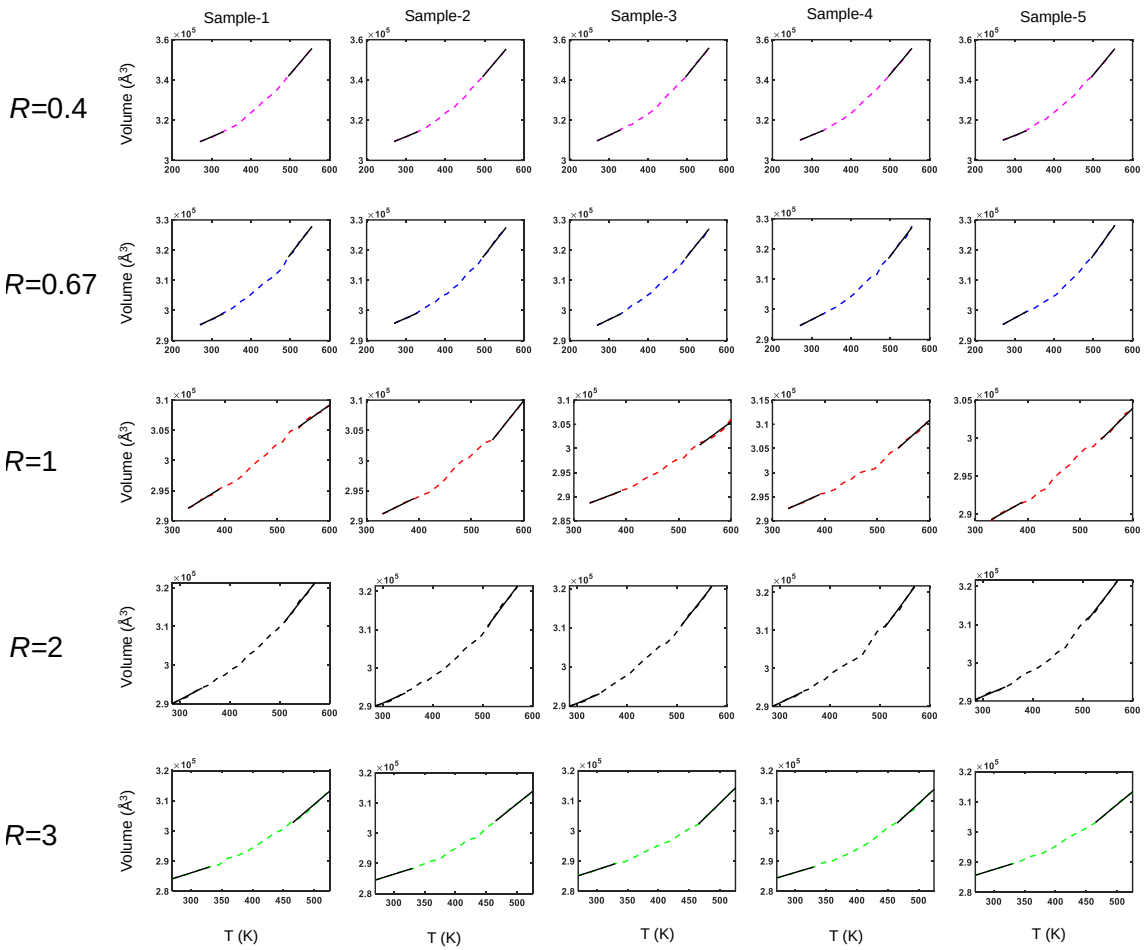

Figure S5: Volume as a function temperature for the systems studied. The black lines represent the linear fit to the rubbery and glassy regime.

S1 Estimation of T_g

Let (T_{gl}, ρ_{gl}) and (T_r, ρ_r) represent a point in the glassy regime and rubbery regime respectively (see Fig. S6). The equation of a line segment in the glassy regime can then be written as

$$\rho_{gl} = \bar{\rho_{gl}} + b_{gl}(T_{gl} - \bar{T_{gl}}) \tag{1}$$

and similarly a line segment in the rubbery regime can be written as

$$\rho_r = \bar{\rho_r} + b_r(T_r - \bar{T_r}) \tag{2}$$

where $(\bar{T_{gl}}, \bar{\rho_{gl}})$ and $(\bar{T_r}, \bar{\rho_r})$ are the centroids of the glassy line segment and the rubbery line segment respectively .

The abscissa of the point of intersection of the two segments given by Eq. 1 and Eq. 2 is then taken to be the T_g and is given by

$$T_g = -\frac{\bar{\rho_{gl}} - \bar{\rho_r} + b_{gl}\bar{T_{gl}} - \bar{b_r}\bar{T_r}}{b_{gl} - b_r} = -\frac{\Delta a}{\Delta b} \tag{3}$$

The four parameters used in the two line segments (Eq. 1 and Eq. 2), $\bar{\rho_{gl}}$, $\bar{\rho_{gl}}$, b_{gl}, b_r are then computed using the equations derived from weighted least squares (WLS) procedure. For brevity, the subscripts r and gl that distinguish the parameters of the rubbery and glassy line segments respectively are dropped in the following equations but is understood to apply to all quantities evaluated.

$$b = \frac{S_{\rho T}}{S_{TT}} \tag{4}$$

$$S_{\rho T} = \sum_i w_i (T - \bar{T})(\rho - \bar{\rho}) \tag{5}$$

$$S_{TT} = \sum_i w_i (T - \bar{T})^2 \tag{6}$$

$$\bar{\rho} = \frac{\sum_i w_i \rho_i}{\sum_i w_i} \tag{7}$$

$$w_i = \frac{1}{Var(\rho_i)} \tag{8}$$

$$\bar{T} = \frac{\sum_i w_i T_i}{\sum_i w_i} \tag{9}$$

$$Var(b) = \frac{1}{S_{TT}} \tag{10}$$

$$Var(\bar{\rho}) = \frac{1}{\sum_i w_i} \tag{11}$$

The sums were taken over the number of data points in the glassy or rubbery regime, as appropriate. The $Var(\rho)$ is the square of the standard deviation of the average density of five independent samples.

Estimating uncertainty (standard deviation) in glasstransition temperature S_{T_g} amounts to estimating the uncertainty in the intersection region of the two linear segments. A procedure that is frequently used in the field of titrimetry was used for this purpose [4]. The assumptions involved in this procedure are discussed in detail in literature [5, 4]. The uncertainty in T_g is calculated as,

$$S_{T_g} = \sqrt{Var(T_g)} \tag{12}$$

and $Var(T_g)$ is given by,

$$Var(T_g) = [Var(\bar{\rho_{gl}}) + Var(\bar{\rho_r}) + \sum_j (\bar{T_j^2} - 2\bar{T_j}T_g + T_g^2)Var(b_j)]/\Delta b^2 \tag{13}$$

where $\sum_j$ implies a sum of two terms, one with subscript j=r and one with j=gl.

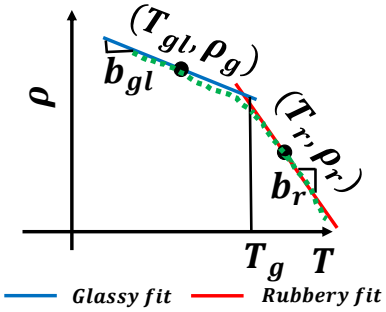

Figure S6: Illustration of T_g estimation procedure. $(\bar{T_{gl}}, \bar{\rho_{gl}})$ and $(\bar{T_r}, \bar{\rho_r})$ are the centroids of the glassy line segment (red) and the rubbery line segment (blue) respectively. T is the temperature, ρ is the density and T_g is the glass transition temperature.

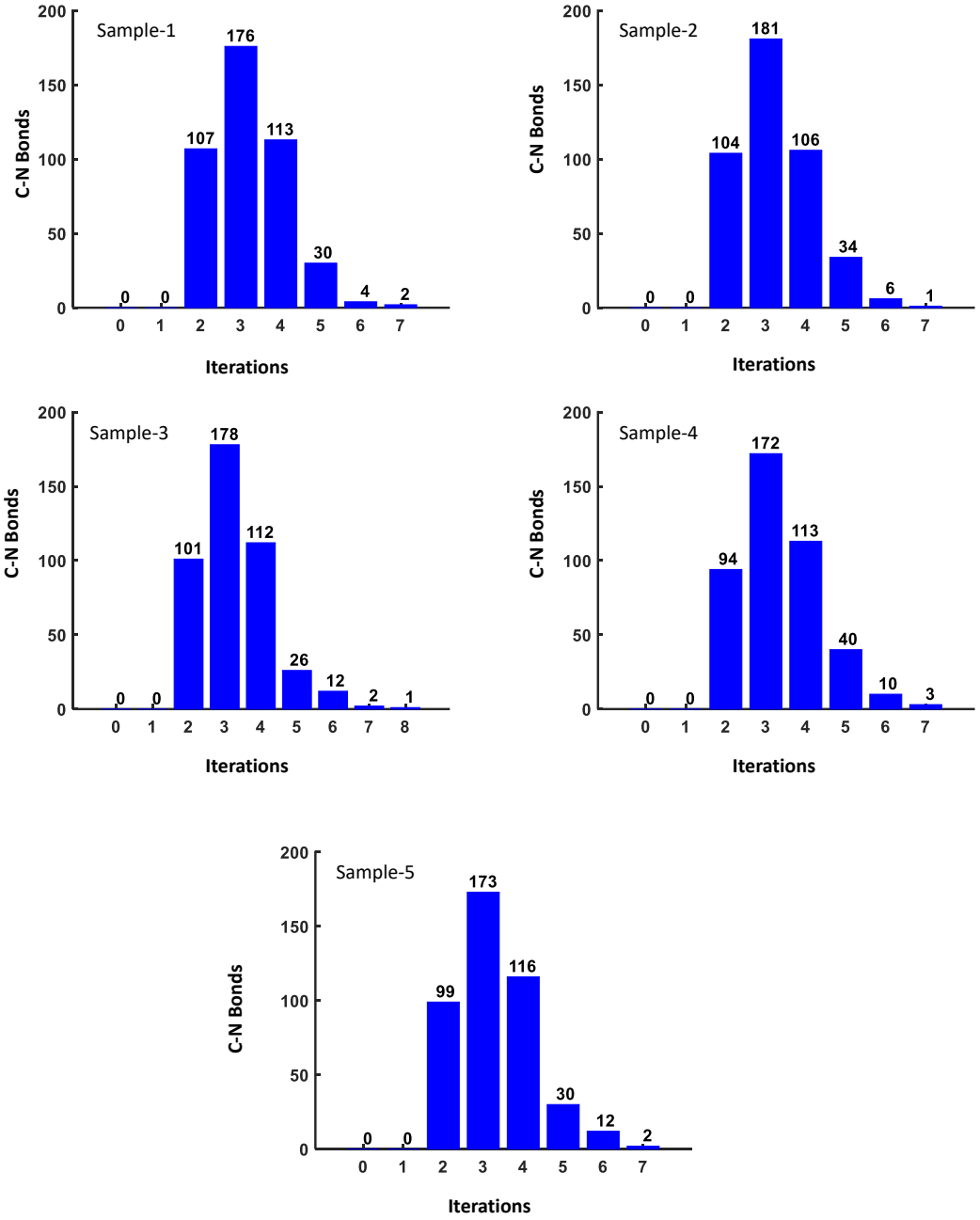

Figure S7: C-N bonds created at each cure iteration in R=0.4 samples

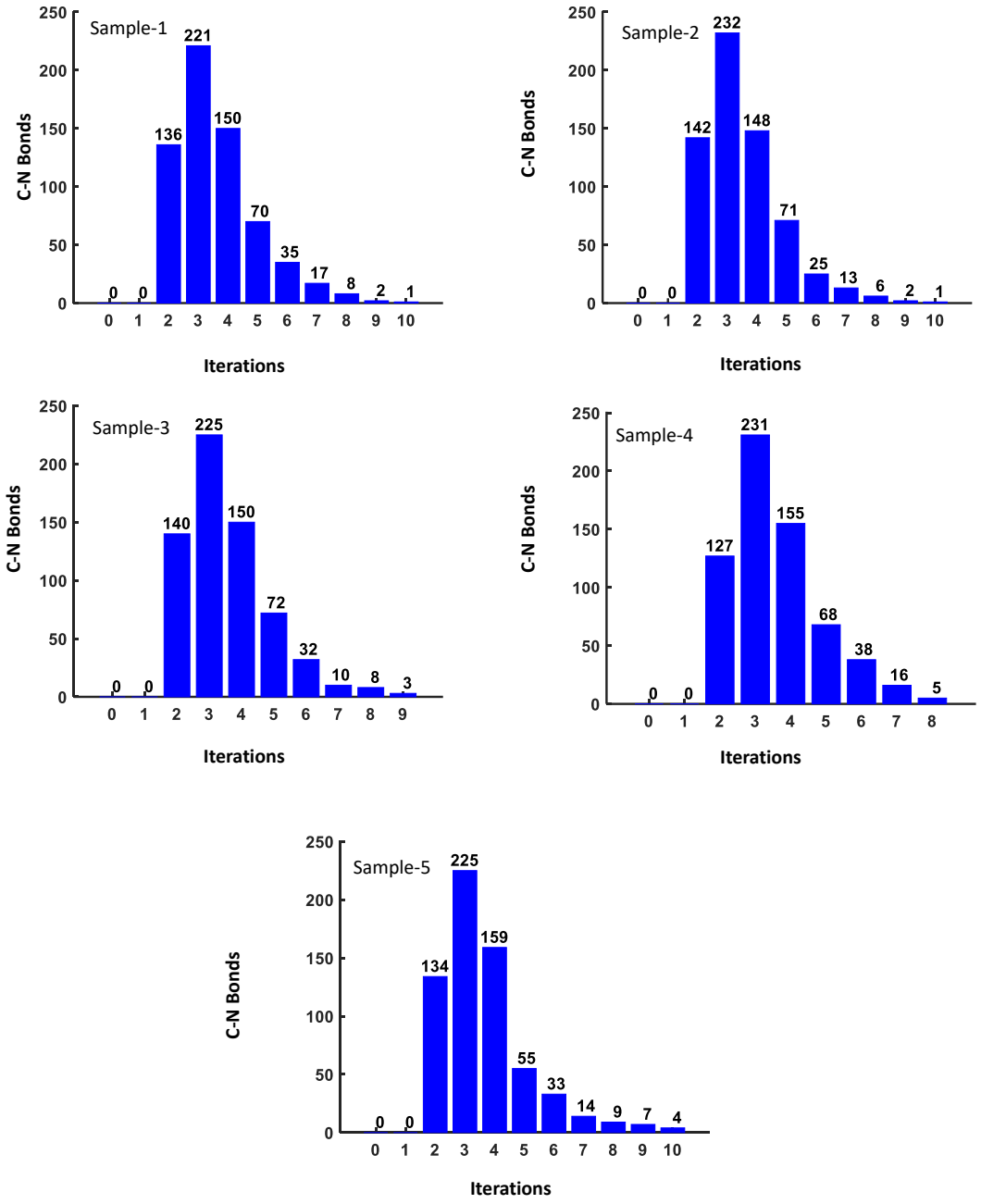

Figure S8: C-N bonds created at each cure iteration in R=0.67 samples

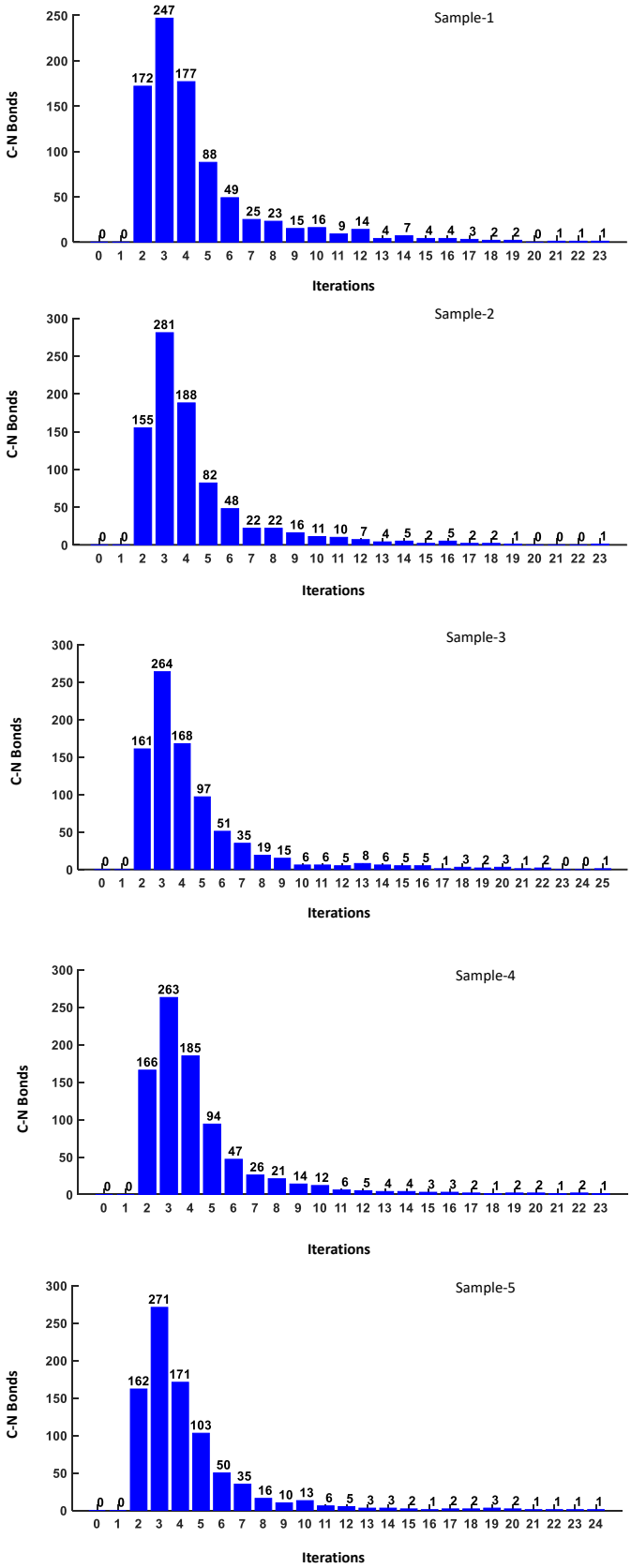

Figure S9: C-N bonds created at each cure iteration in R=1 samples

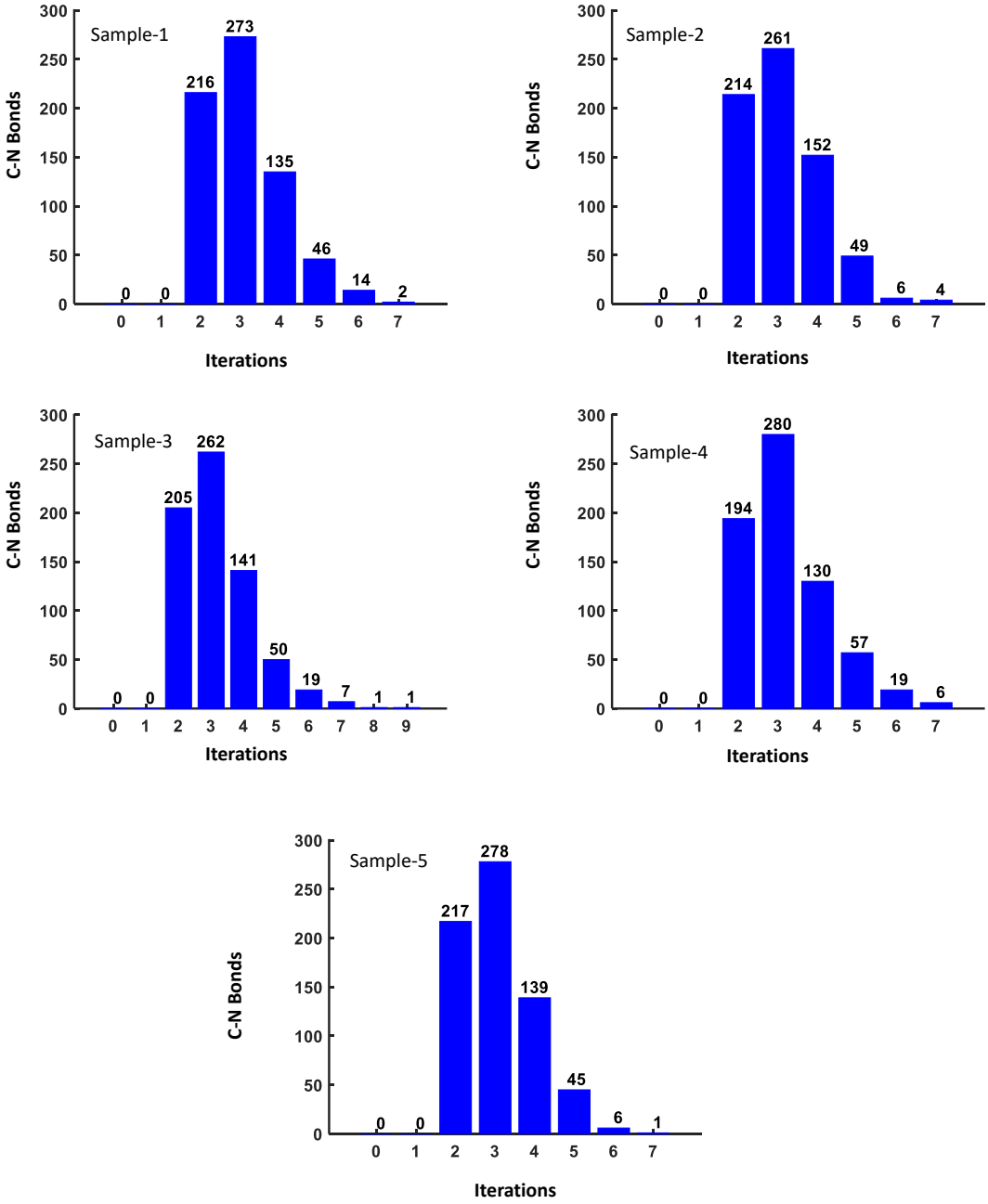

Figure S10: C-N bonds created at each cure iteration in R=2 samples

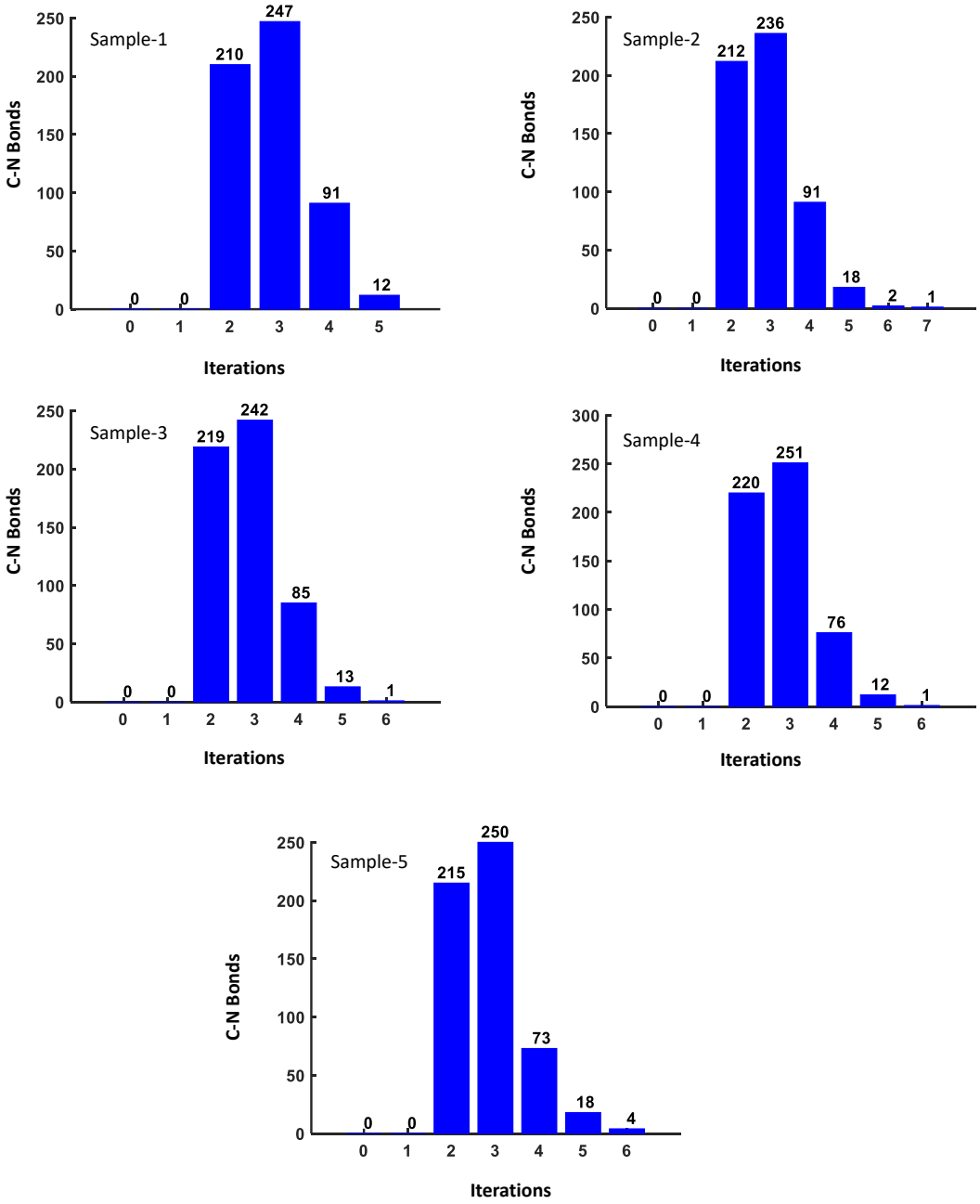

Figure S11: C-N bonds created at each cure iteration in R=3 samples

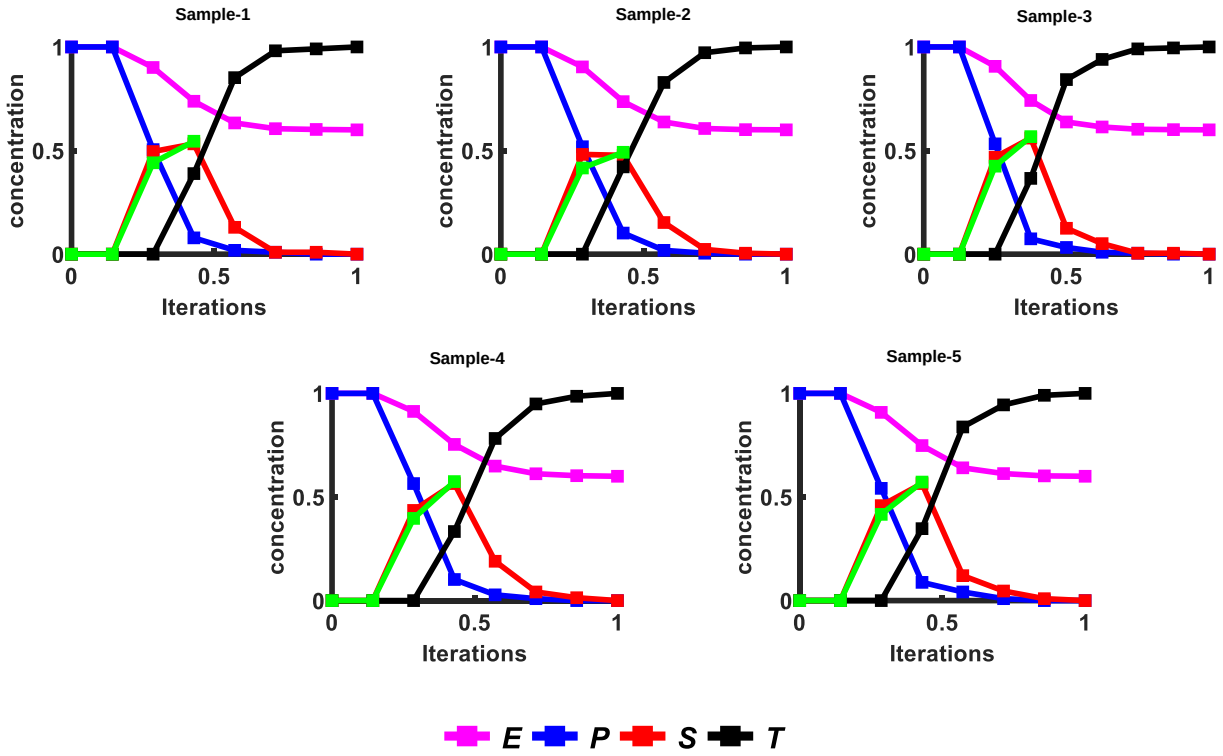

Figure S12: Concentration profiles of functional groups during cure in R=0.4 samples. The green line represents the first order kinetic fit to secondary amine evolution.

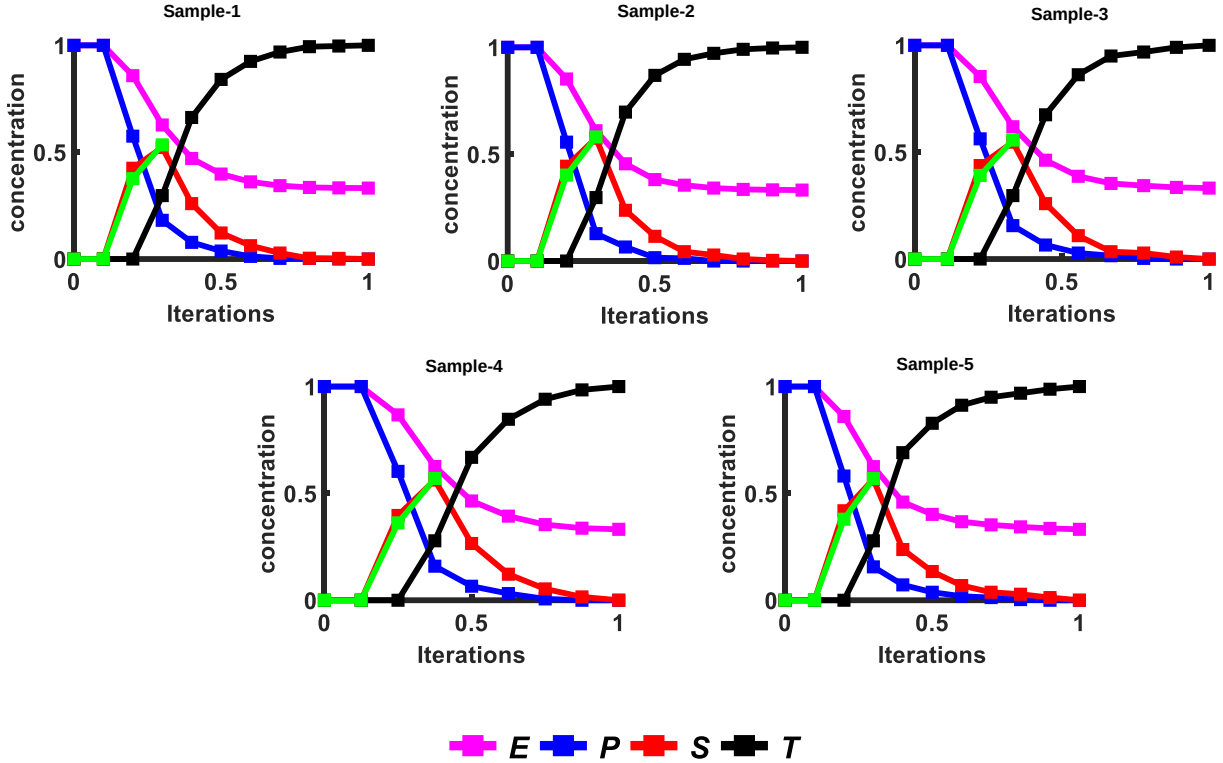

Figure S13: Concentration profiles of functional groups during cure in R=0.67 samples. The green line represents the first order kinetic fit to secondary amine evolution.

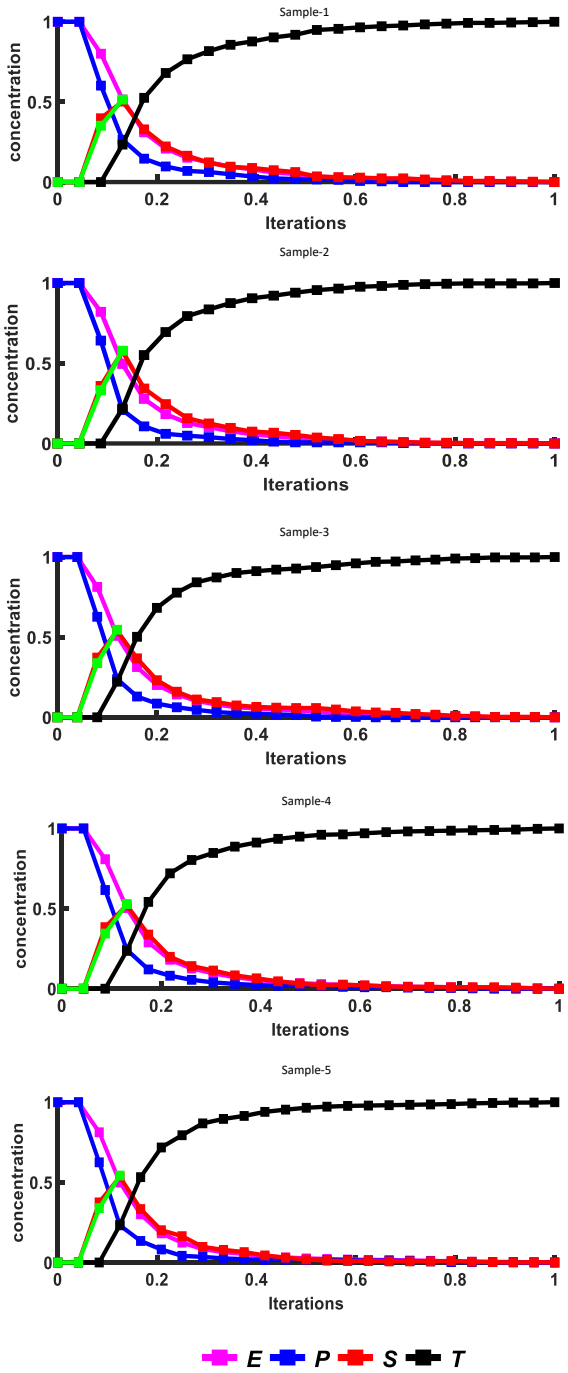

Figure S14: Concentration profiles of functional groups during cure in R=1 samples. The green line represents the first order kinetic fit to secondary amine evolution.

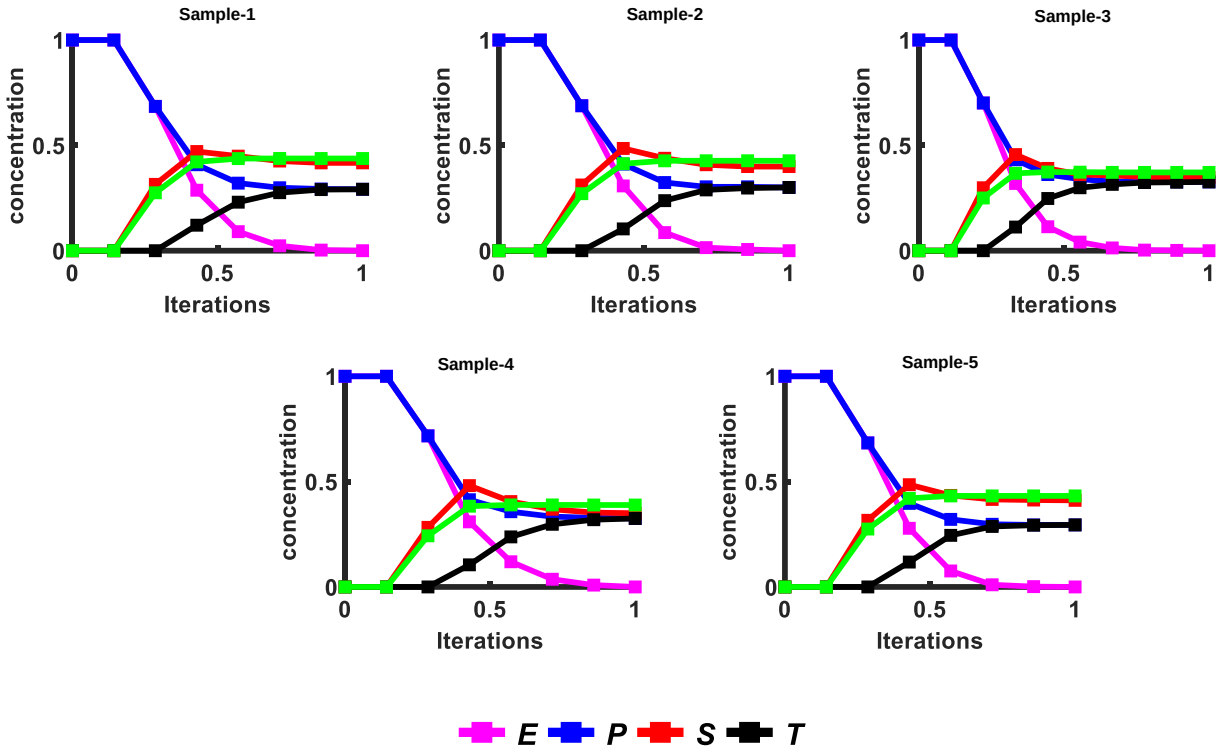

Figure S15: Concentration profiles of functional groups during cure in R=2 samples. The green line represents the first order kinetic fit to secondary amine evolution.

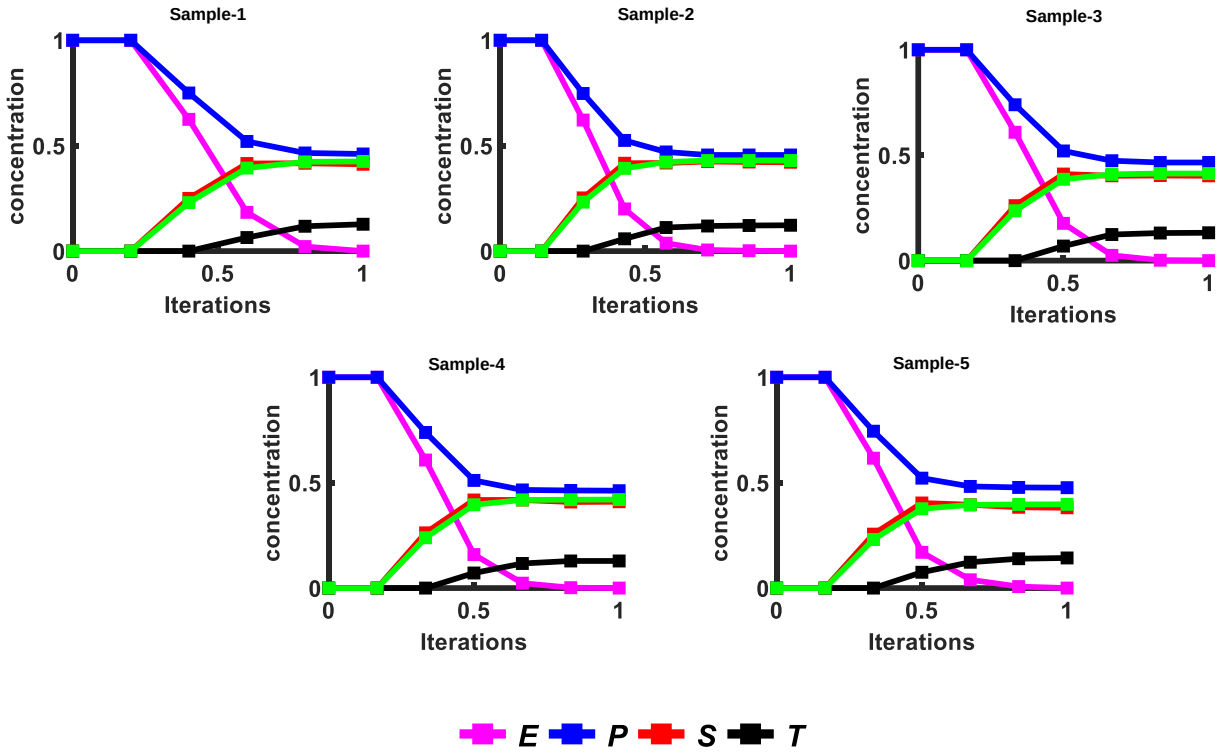

Figure S16: Concentration profiles of functional groups during cure in R=3 samples. The green line represents the first order kinetic fit to secondary amine evolution.

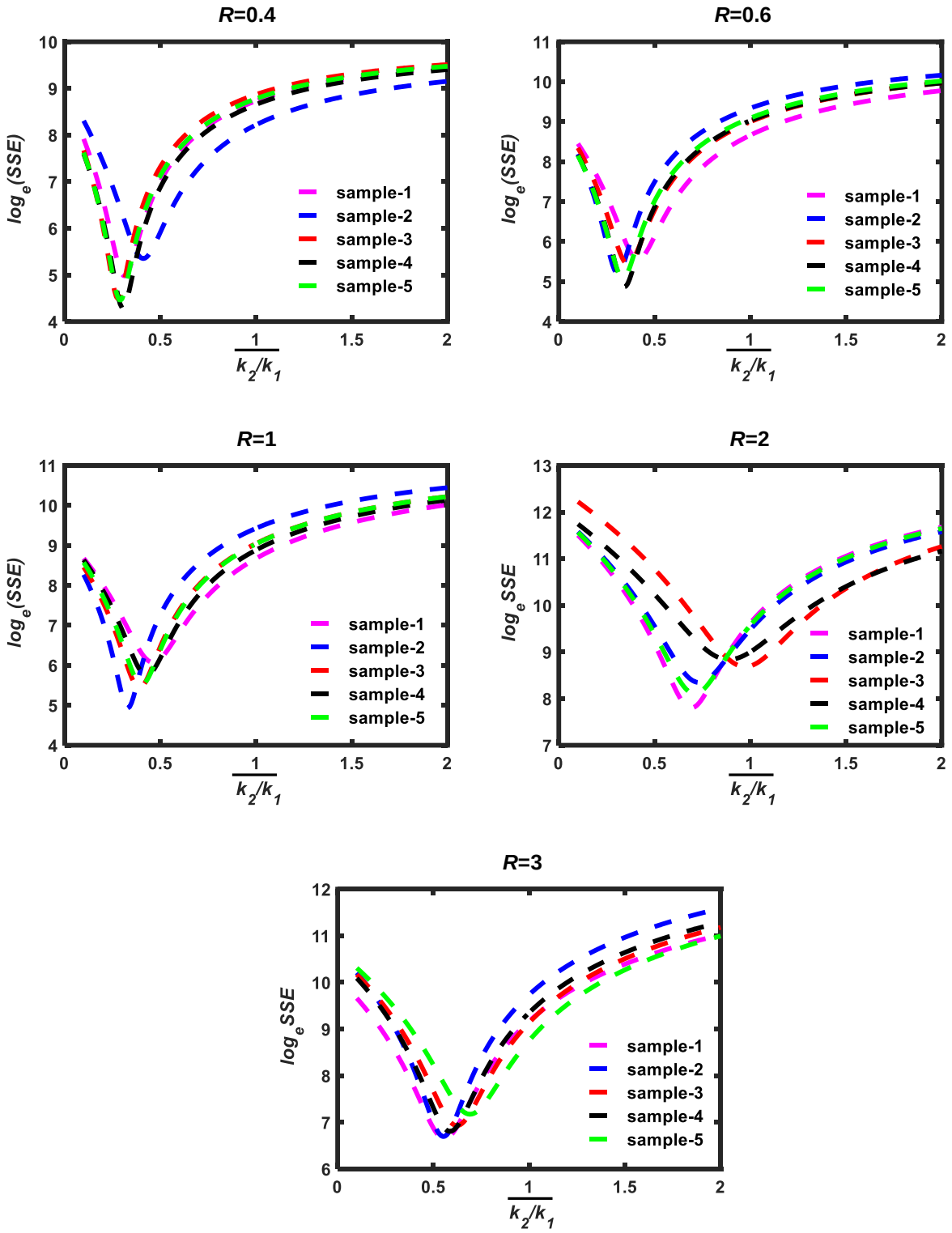

Figure S17: Sum of the squared errors as a function of $\overline{k_2/k_1}$ for the systems studied

System	Glassy range	Rubbery range
R=0.4	270 K - 330 K	495 K - 555 K
R=0.67	270 K - 330 K	495 K - 555 K
R=1	330 K - 390 K	540 K - 600 K
R=2	285 K - 345 K	510 K - 570 K
R=3	270 K - 330 K	465 K - 525 K

Table S2: Temperature ranges used for the estimation of T_g and CVTEs

System	# of atoms before ×	# of atoms after ×	Box edge length (Å) at 210 K
R=0.4	33048	32184	67.361
R=0.67	32000	30720	66.34
R=1	31752	30024	65.87
R=2	32242	30870	65.91
R=3	32060	30940	65.56

Table S3: Simulation box specifications: × stands for crosslinking. The simulation box is cubic. Uncertainties in box lengths are negligible.

Sample	E_0	E_1	E_2	A_0
1	81	270	189	108
2	93	246	201	108
3	90	252	198	108
4	96	240	204	108
5	92	248	200	108

Table S4: Monomer types in R=0.4 system.

Sample	E_0	E_1	E_2	A_0
1	229	182	69	160
2	221	198	61	160
3	226	188	66	160
4	224	192	64	160
5	224	192	64	160

Table S5: Monomer types in R=0.67 system.

Sample	E_0	A_0	A_1	A_2	$A_{2'}$	A_3	A_4
1	343	40	76	60	44	90	33
2	343	33	92	55	48	72	43
3	343	50	75	40	49	83	46
4	343	50	70	43	53	84	43
5	343	40	73	63	49	83	35

Table S6: Monomer types in R=2 system.

Sample	E_0	A_0	A_1	A_2	$A_{2'}$	A_3	A_4
1	280	9	44	65	45	172	85
2	280	8	45	83	42	143	99
3	280	8	44	60	51	174	83
4	280	8	42	76	50	150	94
5	280	8	46	66	58	142	100

Table S7: Monomer types in R=3 system.

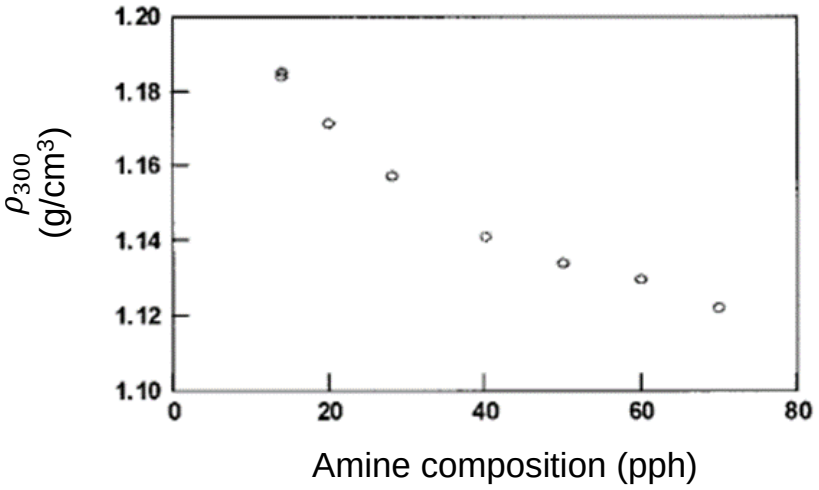

Figure S18: Experimental data on ρ_{300} (room temperature density) as a function of amine composition (reprinted here with permission from reference [1], copyright 1999 John Wiley & Sons.).

R	Amine composition (pph)	T_g (^{0}C)	ρ_{300} (g/cm^3)
0.51	14.3	65	1.183
0.70	19.8	88	1.171
1	28.4	161	1.157
1.44	40.6	120	1.140
1.79	50.2	106	1.133
2.16	60.6	91	1.129
2.50	40.3	78	1.121

Table S8: Experimental data on room temperature density ρ_{300} and glass transition temperature T_g. The values of T_g were taken from reference [1]. The density data were extracted from Fig. S18 using a graphical extraction tool [3]. The amine composition in pph was converted to an equivalent amine-to-epoxy ratio R using the relation, $r = \frac{2M_E}{M_A}\frac{w_a}{w_e}$, where M_E and M_A are the molecular weight of epoxy (375 g/mol) and amine respectively and $\frac{w_a}{w_e}$ is the amine-to-epoxy weight ratio (pph amine)

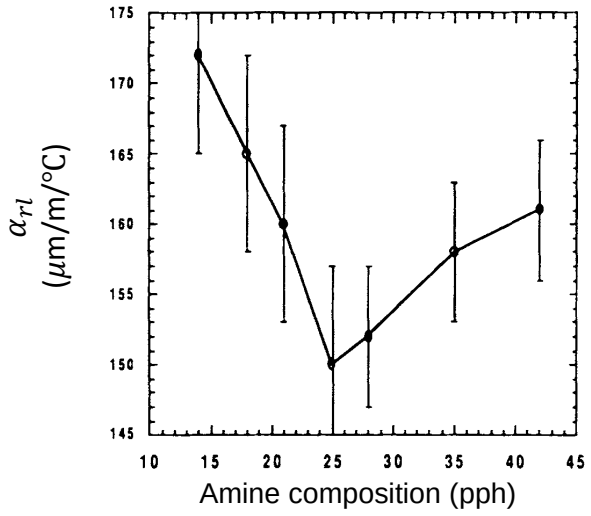

Figure S19: Experimental data on linear thermal expansion coefficient in the rubbery state α_{rl} as a function of amine composition (reprinted here with permission from reference [2], copyright 1992 John Wiley & Sons).

R	Amine composition (pph)	α_{rl} $\mu m/\mathrm{m}/^0\mathrm{C}$
0.5	14	172
0.64	18	165.11
0.76	21.34	160
1	28.09	152.06
1.26	35.43	158
1.66	46.64	161

Table S9: Experimental values of α_{rl}. The data were extracted from Fig. S22 using a graphical extraction tool [3].

S2 Regression models used for estimating missing properties from experimental data

The polynomial model that best fits ρ_{300} vs. R data (Table. S8) is given by,

$$\rho_{300}(R) = a_3R^3 + a_2R^2 + a_1R + a_0 \tag{14}$$

where a_3=-0.0073, a_2=0.0462, a_1=-0.1130 and a_0=1.23.

The polynomial model that best fits T_g vs. R data (Table. S8) is given by,

$$T_g(R) = c_3R^3 + c_2R^2 + c_1R + c_0 \tag{15}$$

where c_3=0, c_2=249.5525, c_1=-180.9058 and c_0=92.3534 for R <1 and c_3=-30.3666, c_2=183.1428 and c_1=-400.3315 and c_0=408.3625 for R >1

The polynomial model that best fits α_{rl} vs. R data (Table. S9) is given by,

$$\alpha_{rl}(R) = b_1R + b_0 \tag{16}$$

where b_1=-39.92 and b_0=191.19 for R <1 and b_1=-39.92 and b_0=191.19 for R >1

R	ρ_{300}(g/cm^3)		T_g(^{0}C)		α_{rl} (μm/m/^{0}C)	
	Sim.	Exp.	Sim.	Exp.	Sim.	Exp.
0.4	1.1062±0.0018	1.19	120.59±0.0036	60	220.67±4.24	175.2
0.67	1.1050±0.0014	1.17	144±0.0046	83.17	173.63±7.17	164.44
1	1.1040±0.0065	1.15	189.71±0.0261	161	90±21	152.06
2	1.0784±0.0011	1.13	161.64±0.0035	97.34	177±6.14	166.19
3	1.0640±0.0025	1.10	137.70±0.0067	35.75	189.74±15.13	179.53

Table S10: Comparison of material properties determined from MD simulations (Sim.) and experimental data (Exp.) from literature. The experimental values of material properties of off-stoichiometric systems ($R \neq 1$) were obtained (estimated) using regression models.

System	T_g^{exp*}(^{0}C)	T_g^{WLF}(^{0}C)	$T_g^{heuristic}$(^{0}C)
R=0.4	60	33	66-88
R=0.67	83.17	56	89-11
R=1	161	102	135-157
R=2	97.34	74	107-129
R=3	35.75	50	83-105

Table S11: The adjusted values of T_g based on shift estimated using WLF equation, T_g^{WLF} and heuristic approach, $T_g^{heuristic}$ and the estimated experimental values of T_g calculated from regression model, T_g^{exp*} (same as in Table. S10, listed here for ease of comparison)

R	w_{Def}	w_{sol}	ϕ_{Def} at 300 K
0.4	0.7420±0.0094	0.3274±0.0094	0.7450±0.0088
0.67	0.4417±0.0051	0.1122±0.0051	0.4459±0.0048
1	0	0	0
2	0.3321±0.0081	0.0442±0.0063	0.3690±0.0083
3	0.4688±0.0005	0.1050±0.0089	0.5147±0.0007

Table S12: Volume fraction of defects, ϕ_{Def} at 300 K, weight fraction of defects, w_{Def} and weight fraction of sols, w_{sol}.

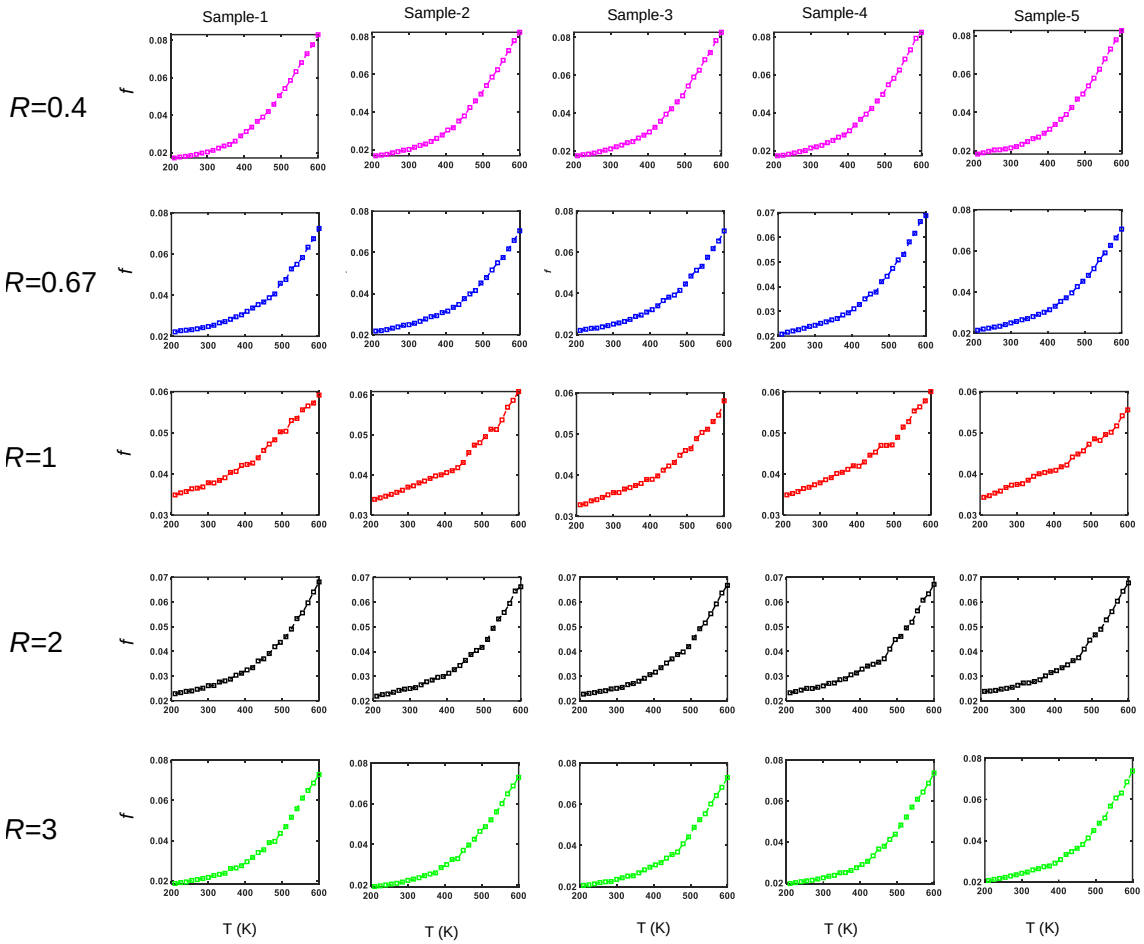

Figure S20: Fractional free volume as a function of temperature for the systems studied.

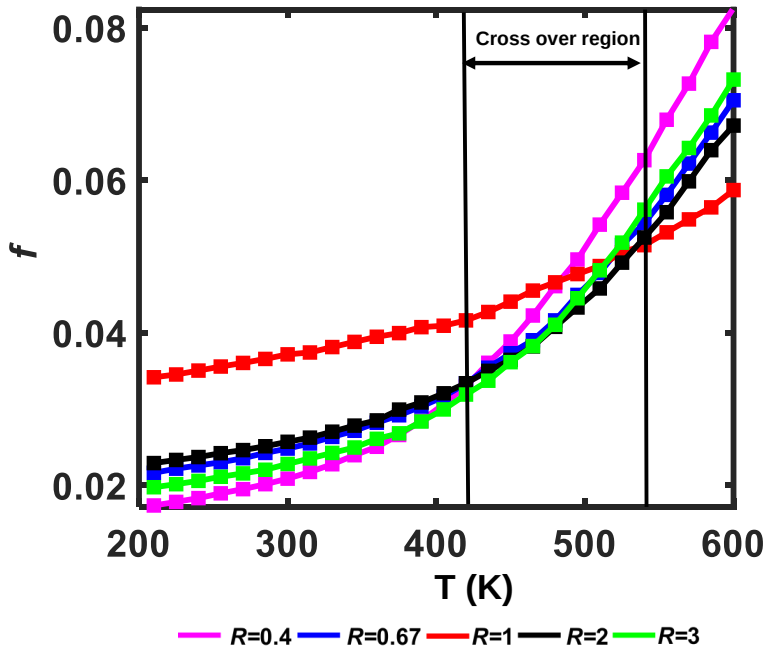

Figure S21: Average fractional free volume as a function of temperature for the systems studied. The temperature range over which crossover in the trend i.e., increase in fractional volume to decrease in fractional volume, for deviations from R=1, occurs is shown.

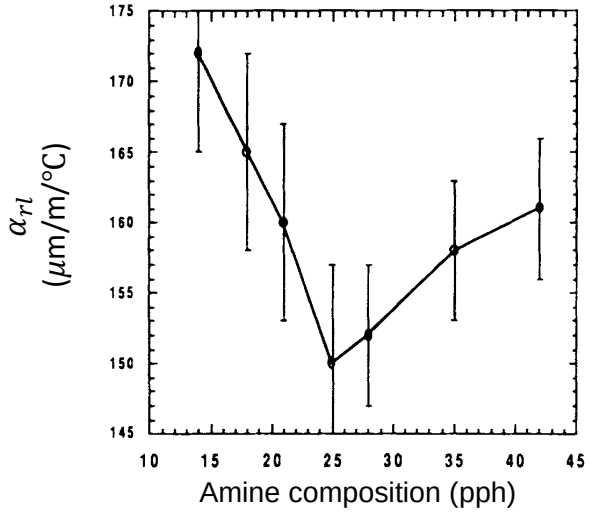

Figure S22: Experimental data on linear thermal expansion coefficient in the rubbery state α_{rl} as a function of amine composition (reprinted here with permission from reference [2], copyright 1992 John Wiley & Sons).

S3 Data availability

The LAMMPS data files of the systems and description on how to visualize the monomer types and crosslinks (C-N bonds) can be found in a zipped folder which can downloaded via the link provided below. The folder also contains mol2 files of epoxy and amine which contain the partial charges. More data can be provided on reasonable request.

https://www.dropbox.com/s/aeeijqgcw3tdf8d/SI_DGEBAPACM.zip?dl=0

References

[1] M. R. Vanlandingham, R. F. Eduljee, and J. W. Gillespie Jr. Relationships between stoichiometry, microstructure, and properties for amine-cured epoxies. *Journal of Applied Polymer Science*, 71(5):699–712, 1999.

[2] G. R. Palmese and R. L. McCullough. Effect of epoxy–amine stoichiometry on cured resin material properties. *Journal of Applied Polymer Science*, 46(10):1863–1873, 1992.

[3] Ankit Rohatgi. Webplotdigitizer: Version 4.2, 2019.

[4] Lowell M. Schwartz and Robert I. Gelb. Statistical uncertainties of end points at intersecting straight lines. *Anal. Chem.*, 56(8):1487–1492, 1984.

[5] Julia Martin, Gabriel Delgado Martin, and Agustin G. Asuero. Intersecting straight lines: Titrimetric applications. In Vu Dang Hoang, editor, *Advances in Titration Techniques*, chapter 3. IntechOpen, Rijeka, 2017.